



Dehydrogenation Performances of Different Al Source Composite Systems of $2\text{LiBH}_4 + \text{M}$ ($\text{M} = \text{Al}$, LiAlH_4 , Li_3AlH_6)

Yun Li^{1,2}, Shaolong Wu^{1*}, Dongdong Zhu^{3*}, Jun He⁴, Xuezhong Xiao² and Lixin Chen²

¹ School of Mechanical and Electrical Engineering, Quzhou College of Technology, Quzhou, China, ² Key Laboratory of Advanced Materials and Applications for Batteries of Zhejiang Province, Zhejiang University, Hangzhou, China, ³ School of Mechanical Engineering, Quzhou University, Quzhou, China, ⁴ Quzhou Special Equipment Inspection Center, Quzhou, China

OPEN ACCESS

Edited by:

Guanglin Xia,
Fudan University, China

Reviewed by:

Jian Zhang,
Changsha University of Science and
Technology, China
Hujun Cao,
Chinese Academy of Sciences, China

*Correspondence:

Shaolong Wu
shanxiliyun2006@163.com
Dongdong Zhu
zhudd8@163.com

Specialty section:

This article was submitted to
Inorganic Chemistry,
a section of the journal
Frontiers in Chemistry

Received: 19 February 2020

Accepted: 10 March 2020

Published: 15 April 2020

Citation:

Li Y, Wu S, Zhu D, He J, Xiao X and
Chen L (2020) Dehydrogenation
Performances of Different Al Source
Composite Systems of $2\text{LiBH}_4 + \text{M}$
($\text{M} = \text{Al}$, LiAlH_4 , Li_3AlH_6).
Front. Chem. 8:227.
doi: 10.3389/fchem.2020.00227

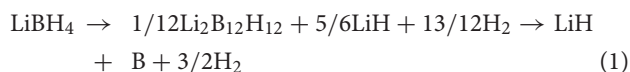
Hydrogen has become a promising energy source due to its efficient and renewable properties. Although promising, hydrogen energy has not been in widespread use due to the lack of high-performance materials for hydrogen storage. Previous studies have shown that the addition of Al-based compounds to LiBH_4 can create composites that have good properties for hydrogen storage. In this work, the dehydrogenation performances of different composite systems of $2\text{LiBH}_4 + \text{M}$ ($\text{M} = \text{Al}$, LiAlH_4 , Li_3AlH_6) were investigated. The results show that, under a ball to powder ratio of 25:1 and a rotation speed of 300 rpm, the optimum ball milling time is 50 h for synthesizing Li_3AlH_6 from LiH and LiAlH_4 . The three studied systems destabilized LiBH_4 at relatively low temperatures, and the $2\text{LiBH}_4\text{-Li}_3\text{AlH}_6$ composite demonstrated excellent behavior. Based on the differential scanning calorimetry results, pure LiBH_4 released hydrogen at 469°C . The dehydrogenation temperature of LiBH_4 is 416°C for $2\text{LiBH}_4\text{-Li}_3\text{AlH}_6$ versus 435°C for $2\text{LiBH}_4\text{-LiAlH}_4$ and 445°C for $2\text{LiBH}_4\text{-Al}$. The $2\text{LiBH}_4\text{-Li}_3\text{AlH}_6$, $2\text{LiBH}_4\text{-LiAlH}_4$, and $2\text{LiBH}_4\text{-Al}$ samples released 9.1, 8, and 5.7 wt.% of H_2 , respectively. Additionally, the $2\text{LiBH}_4\text{-Li}_3\text{AlH}_6$ composite released the 9.1 wt.% H_2 within 150 min. An increase in the kinetics was achieved. From the results, it was concluded that $2\text{LiBH}_4\text{-Li}_3\text{AlH}_6$ exhibits the best dehydrogenation performance. Therefore, the $2\text{LiBH}_4\text{-Li}_3\text{AlH}_6$ composite is considered a promising hydrogen storage material.

Keywords: hydrogen storage materials, LiBH_4 , composite system, $2\text{LiBH}_4\text{-Li}_3\text{AlH}_6$, dehydrogenation performance

INTRODUCTION

Hydrogen energy has become an ideal new energy resource due to its clean, efficient, and renewable properties (Schlapbach and Zuttel, 2001). Although the use of hydrogen energy is promising, widespread use has been hindered by issues in the advancement of high-performance materials for hydrogen storage (Liu et al., 2010). The complex hydride (Ley et al., 2014) LiBH_4 , which has

a hydrogen capacity storage of 18.5 wt.%, has drawn extensive attention. LiBH_4 decomposes into an intermediate compound $\text{Li}_2\text{B}_{12}\text{H}_{12}$, which generates B and releases H_2 as described in Equation (1) (Orimo et al., 2006).



However, many factors impede the commercial application of pure LiBH_4 , such as high dehydrogenation temperature, slow dehydrogenation rate, and poor cycle reversibility (Lodziana and Vegge, 2004). To solve these issues, researchers have concentrated on modifying LiBH_4 (Vajo and Olson, 2007) through anion/cation substitution (Fang et al., 2011; Lombardo et al., 2019), catalytic modification (Kou et al., 2012; Huang et al., 2016; Zhai et al., 2016), the combined effect of composites (Vajo et al., 2010; Kou et al., 2012), and the application of the confinement effect of nano-materials (Vajo, 2011; Zhang et al., 2017).

Al and Al-based composites with LiBH_4 are of interest. Founded on first-principles calculation, Siegel et al. (2007) predicted that LiBH_4 would react with Al to generate AlB_2 , LiH, and H_2 at 280°C under a hydrogen pressure of 1 bar. For the LiAlH_4 - LiBH_4 system, Mao et al. (2009) found that the addition of TiF_3 decreased the onset temperatures of H_2 release by 64 and 150°C compared with the undoped system. The decomposition enthalpy values of LiBH_4 also reduced to 60.4 kJ/mol. He et al. (2019) studied the dehydrogenation performance of $\text{LiBH}_4/\text{LiAlH}_4$ composite, found that 8.7 wt.% of hydrogen was released at 500°C , and defined a "Li-Al-B-H" compound. Soru et al. (2014) focused on the phase structural transformation of the $\text{LiAlH}_4 + \text{LiBH}_4$ system, which can produce 6.8 wt.% of hydrogen. According to a study by Carrillo-Bucio et al. (2017), a surface-oxidized $2\text{LiBH}_4 + \text{Al}$ composite did not release hydrogen until heated to 400°C under a 3 bar initial backpressure. With the catalytic effect of TiF_3 , the mixture obtained 9.3 wt.% of hydrogen release as compared to the 5.8 wt.% of the undoped mixture. In research by Zhang et al. (2018), a combined mixture of MgH_2 , LiBH_4 , and LiAlH_4 showed superior performance, starting to release hydrogen at 280°C and maintaining reversibility. In our previous studies (Li et al., 2012), the dehydrogenation temperatures of $2\text{LiBH}_4 + \text{Li}_3\text{AlH}_6$ doped with titanium were decreased by 80 and 50°C , respectively, vs. the undoped system. From the previous studies, it can be summarized that Al can enhance the hydrogen storage performance of LiBH_4 to some extent. However, the dehydrogenation behaviors of different Al source composite systems have not been systematically studied. In this work, three Al-based LiBH_4 composite systems, 2LiBH_4 -Al, 2LiBH_4 - LiAlH_4 , and 2LiBH_4 - Li_3AlH_6 were prepared, and the hydrogen storage performance was investigated.

MATERIALS AND METHODS

Table 1 shows the raw materials used in this study. All powders were carefully stored in a glove box (MIKROUNA), in which

TABLE 1 | Raw materials used in the study.

Materials	LiBH_4	Al	LiAlH_4	LiH
Purity (%)	≥ 95	≥ 99	≥ 95	≥ 98
State	Powder	Powder	Powder	Powder
Supplier	Acros	Sinopharm	Sigma-Aldrich	Sigma-Aldrich

noble gas was loaded and the oxygen content and water vapor content were kept below 1 ppm. A planetary mill (QM-3SP2) was utilized to prepare the composites.

The dehydrogenation properties of the materials were tested with a Sievert-type device. The changes in temperature and pressure over time were recorded. The ideal gas state equation was utilized to calculate the dehydrogenation capacity. Thermal analysis was performed using differential scanning calorimetry (DSC, Netzsch 449C Jupiter) combined with thermogravimetric analysis (TG, QMS 403C). To protect the samples from oxidation, high purity argon gas was added at a flow rate of 50 mL/min. An empty aluminum crucible was used as a reference during analysis. The phase compositions of the samples were determined by X-ray powder diffraction (X'Pert-PRO, PANalytical); its scanning range (2θ) was 15° - 80° . A specific sealed device was used to protect samples from being oxidized or damped during analysis. Fourier transform infrared spectroscopy (FTIR, Tensor 27) was employed to detect some amorphous substances with a scanning rate of $30\text{ cm}^{-1}/\text{min}$ and a resolution ratio of 0.5 cm^{-1} .

RESULTS AND DISCUSSION

Preparation of Li_3AlH_6 Powder

In this work, Li_3AlH_6 powder was synthesized *in-situ* by ball milling LiH and LiAlH_4 . Approximately 15 g mixed powder of LiH and LiAlH_4 was milled each time with a molar ratio of 2:1, a ball to powder ratio of 25:1, and a milling speed of 300 rpm. To suppress temperature rise in the ball milling, every 30 min was set as an operation cycle, which contained a stop time of 6 min, periodically. After ball milling for 20 h, XRD patterns were obtained and examined to characterize the mixed powder. **Figure 1** shows the XRD results of pure LiH powder, LiAlH_4 powder, and the LiH and LiAlH_4 powder after ball milling for 20 h. No impurity phases were observed in any of the samples, which indicates that the samples were highly pure and did not oxidize. As shown in **Figure 1C**, a few Li_3AlH_6 diffraction peaks are present, while the rest are of LiAlH_4 and LiH. This shows that the synthesis reaction was not completed. Due to long milling time, LiH peaks were much lower than before. The LiH content was lower, and an amorphous structure was formed.

Further ball milling was carried out since the synthesis reaction to Li_3AlH_6 was not completed. The milling samples were taken for XRD analysis after every 10 h. **Figure 2** shows the XRD results of the milled powders after 20, 30, 40, and 50 h. Strong double peaks at 22° and 23° are detected, which are the characteristic peaks of Li_3AlH_6 . After ball milling for 30 h, most of the diffraction peaks are Li_3AlH_6 ; however, some LiAlH_4 and

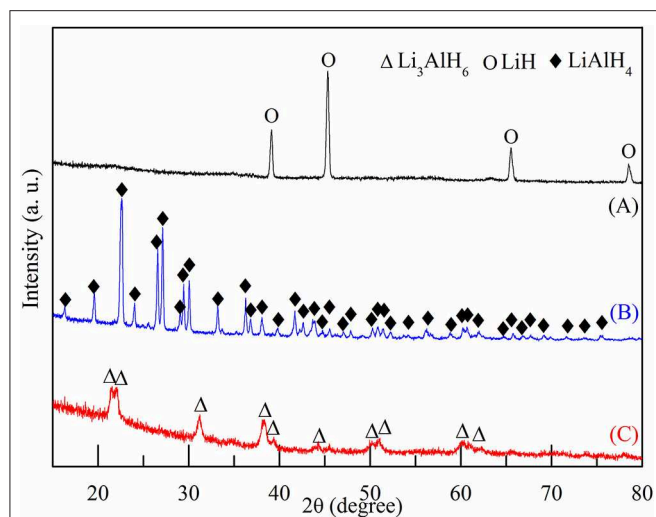


FIGURE 1 | XRD patterns of (A) pure LiH, (B) pure LiAlH₄, and (C) mixed powder of LiH and LiAlH₄ after ball milling for 20 h.

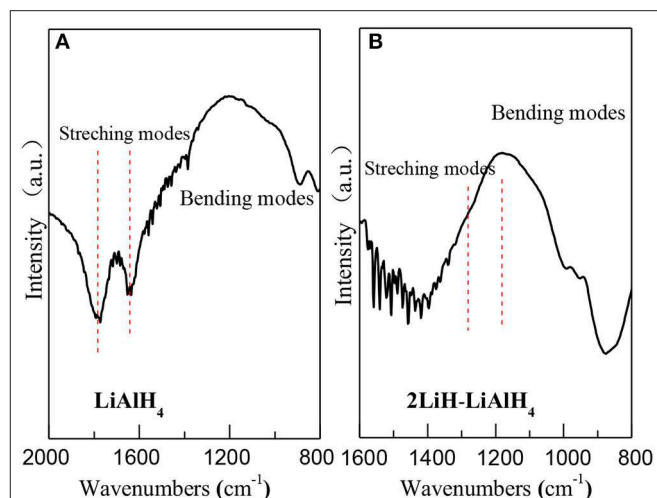


FIGURE 3 | FT-IR spectrums of (A) pure LiAlH₄ and (B) 2LiH-LiAlH₄ mixed powder after 50-h ball milling.

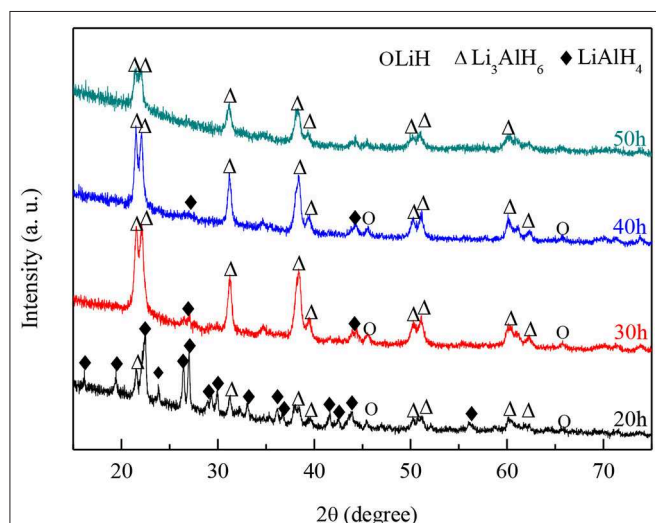


FIGURE 2 | XRD patterns of mixed powder of LiH and LiAlH₄ after ball-milling for different numbers of hours.

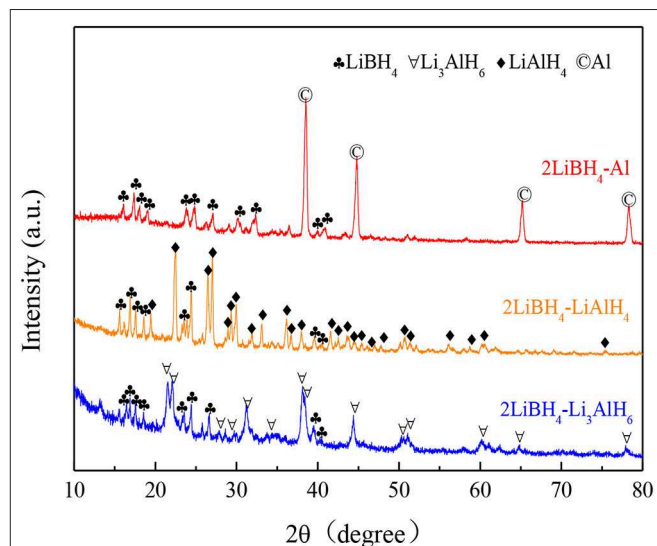


FIGURE 4 | XRD patterns of 2LiBH₄-Al, 2LiBH₄-LiAlH₄, and 2LiBH₄-Li₃AlH₆ mixtures after ball milling for 1 h.

LiH peaks can still be found at 27°, 43°, and 46°. As the ball milling time increased, the LiH and LiAlH₄ content decreased, which shows that the synthesis reaction proceeds as the milling time increases. Nevertheless, the diffraction intensity of Li₃AlH₆ decreased, which shows that the longer milling time, the more likely the production of an amorphous phase becomes.

FTIR analysis was used to investigate the synthesized powder. In pure LiAlH₄ (Figure 3A), the bending modes around 1,780 and 1,610 cm⁻¹ correspond to the A-H stretching band, as was previously shown by Chen et al. (2001). After 50 h ball milling, this A-H stretching band disappeared in the 2LiH-LiAlH₄ mixtures (Figure 3B). A new A-H stretching band was generated around 1,380 cm⁻¹, which belongs to Li₃AlH₆. This indicates the completion of the synthesis reaction.

Characterization of the Composite Samples

The 2LiBH₄ + M (M = Al, LiAlH₄, Li₃AlH₆) composite systems were prepared by ball milling, respectively. The ball-milling time was 1 h, with a mole ratio of 2:1. The as-milled mixtures are presented in Figure 4. In the 2LiBH₄-Al composite, the narrow and sharp diffraction peaks are of Al, while the other diffraction peaks are of LiBH₄. The intensity of the LiAlH₄ peaks in the 2LiBH₄-LiAlH₄ composite are also strong, but both LiBH₄ and Li₃AlH₆ have attenuated diffraction peaks in 2LiBH₄-Li₃AlH₆. The absence of other peaks indicated that there were no side reactions that could generate impurities or by-products during ball milling.

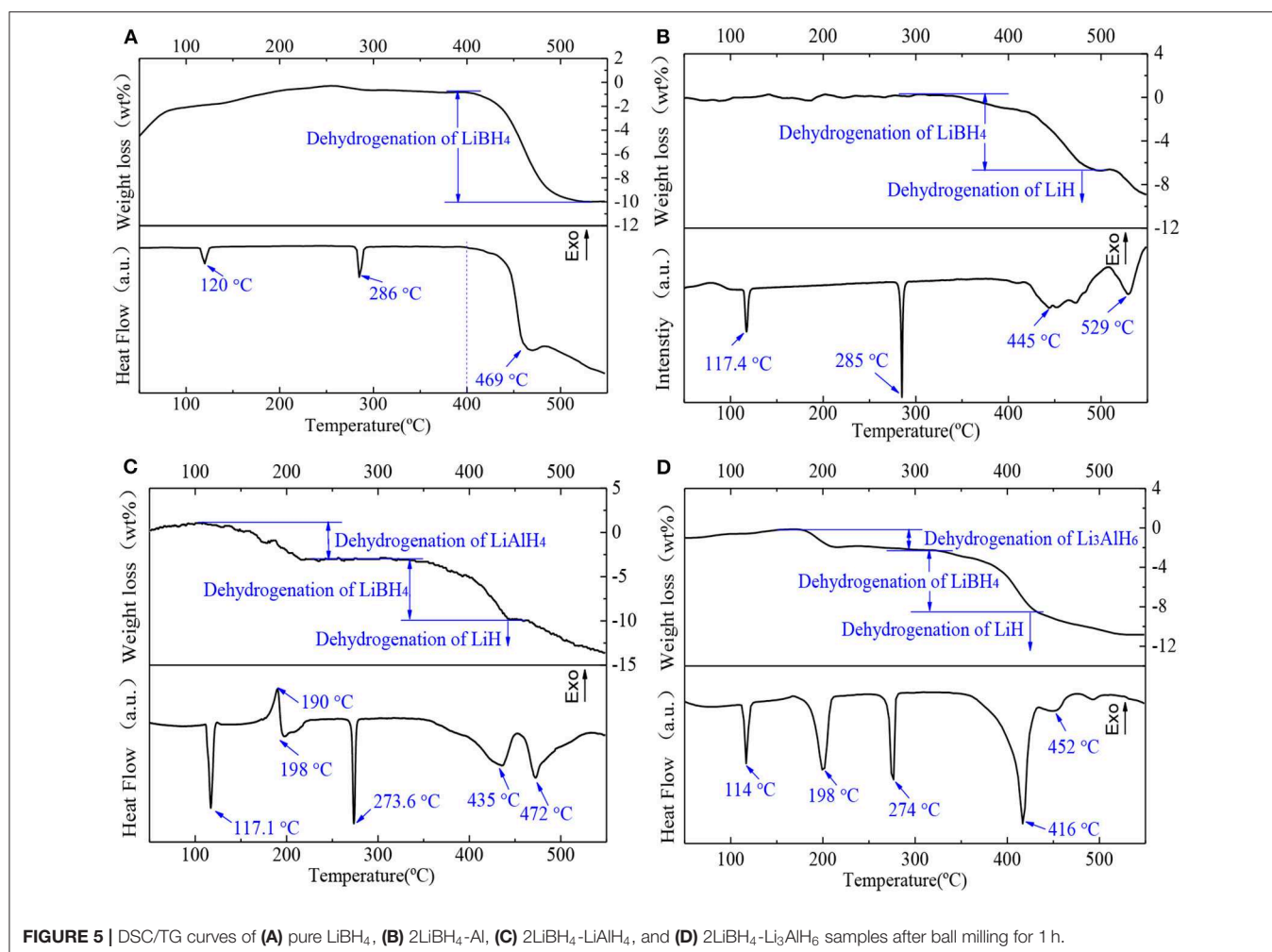


FIGURE 5 | DSC/TG curves of (A) pure LiBH₄, (B) 2LiBH₄-Al, (C) 2LiBH₄-LiAlH₄, and (D) 2LiBH₄-Li₃AlH₆ samples after ball milling for 1 h.

Dehydrogenation Performances

The dehydrogenation performances of the samples were investigated. The four samples were heated to 550°C at a heating rate of 5°C/min in an argon atmosphere. The DSC/TG results are shown in **Figure 5**. In the pure LiBH₄ sample (**Figure 5A**), the endothermic peak at 120°C denotes that LiBH₄ transformed from an orthorhombic to a hexagonal crystal system. The endothermic peak at 286°C is attributed to the melting of LiBH₄. According to the TG curve, LiBH₄ began to release hydrogen and lose weight at 400°C. There is a dehydrogenation peak at around 469°C, and the rate of dehydrogenation slowed down after that. Both the transformation and the melting peak of LiBH₄ for each composite sample are shown in **Figures 5B–D**. All samples have lower transformation and melting temperatures than pure LiBH₄ (transformation temperature: $T_d < T_c < T_b < T_a$; melting temperature: $T_c < T_d < T_b < T_a$). In the as-milled 2LiBH₄-Al sample (**Figure 5B**), the wide endothermic range around 445°C represents the decomposition of LiBH₄. The last peak at 529°C is the decomposition of LiH. As shown in **Figure 5C**, peaks at 190 and 198°C indicated the dehydrogenation of LiAlH₄, which were verified in our previous study (Li et al., 2012). LiAlH₄ decomposed into Li₃AlH₆ at 190°C, and Li₃AlH₆ started to generate LiH, Al, and release H₂ at 198°C. LiBH₄ and LiH started

to decompose at 435 and 472°C, respectively. **Figure 5D** shows that the decomposition peak of Li₃AlH₆ is at 198°C, which is consistent with the 2LiBH₄-LiAlH₄ sample. The decomposition peak of LiBH₄ (416°C) is lower than that of the 2LiBH₄-LiAlH₄ (435°C) or 2LiBH₄-Al samples (445°C). In addition, the decomposition peak of LiH, which is around 452°C, is also lower than that of the other composite systems. These results showed that the LiBH₄ became more unstable due to the addition of Li₃AlH₆ and that hydrogen was released at a lower temperature. The main reason for this is that the Al present in Li₃AlH₆ was active enough to stimulate the dehydrogenation reaction.

The temperature-programmed desorption (TPD) method was implemented to study the dehydrogenation performance of pure LiBH₄, 2LiBH₄-Al, 2LiBH₄-LiAlH₄, and 2LiBH₄-Li₃AlH₆; the results are shown in **Figure 6**. The samples were heated to 400°C and held for 5 h. The pure LiBH₄ began to release H₂ at around 400°C. Its desorption rate slowed down when 5 wt.% of H₂ had been released. The 2LiBH₄-Li₃AlH₆ sample released 9.1 wt.% H₂ within 150 min, which is the fastest reaction kinetics in this work. Its decomposition process includes two main steps, with the release of 3 and 6.1 wt.% H₂ as the first and second steps, respectively. In the 2LiBH₄-LiAlH₄ sample, LiAlH₄ began to decompose at ~130°C and released 3.9 wt.% H₂. Subsequently,

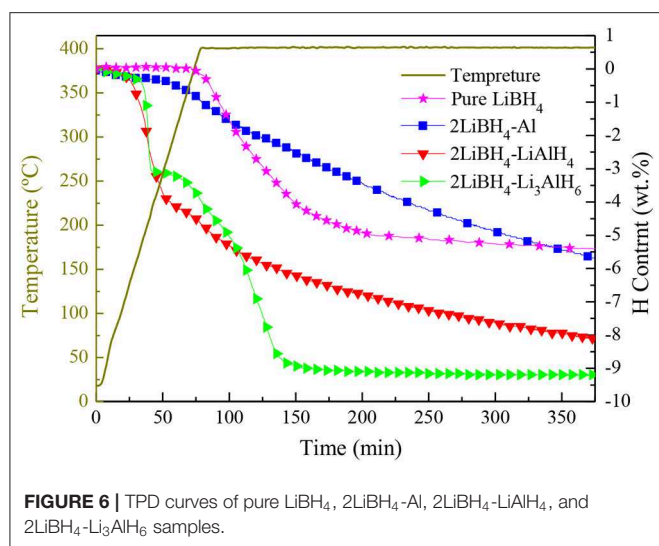


FIGURE 6 | TPD curves of pure LiBH_4 , $2\text{LiBH}_4\text{-Al}$, $2\text{LiBH}_4\text{-LiAlH}_4$, and $2\text{LiBH}_4\text{-Li}_3\text{AlH}_6$ samples.

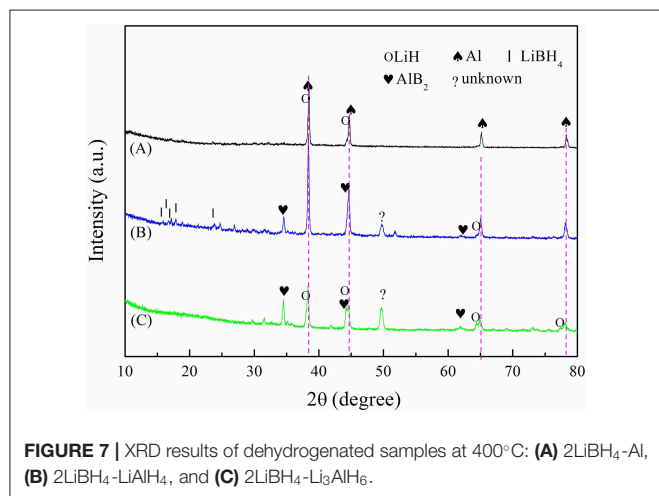


FIGURE 7 | XRD results of dehydrogenated samples at 400°C : (A) $2\text{LiBH}_4\text{-Al}$, (B) $2\text{LiBH}_4\text{-LiAlH}_4$, and (C) $2\text{LiBH}_4\text{-Li}_3\text{AlH}_6$.

its desorption rate was retarded. This composite released a total of 8 wt.% H_2 . The $2\text{LiBH}_4\text{-Al}$ composite had a slower desorption rate. Only 5.7 wt.% H_2 was released after 6 h, which is much lower than the 8.6 wt.% predicted by theoretical capacity. Previous research (Friedrichs et al., 2009) has reported that Al is an effective catalyst to activate LiBH_4 , and this phenomenon can also be observed in this study. However, the Al element generated from $2\text{LiBH}_4\text{-Li}_3\text{AlH}_6$ is much more effective than for the other samples. Since aluminum can be easily oxidized, an oxide film can easily form on the surface of the Al powder, which can slow down the dehydrogenation kinetics. In contrast, the Al in $2\text{LiBH}_4\text{-Li}_3\text{AlH}_6$, decomposed from Li_3AlH_6 exhibits high purity and is non-oxidized, resulting in the superior reaction kinetics of LiBH_4 .

Characterization of the Dehydrogenation Materials

The XRD patterns of the dehydrogenated samples are shown in Figure 7. In Figure 7A, prominent diffraction peaks of LiH and Al are present. However, the LiBH_4 phase was not observed,

as its diffraction intensity is relatively weaker. In Figure 7B, residual peaks of LiBH_4 are observed, which demonstrates incomplete dehydrogenation. In Figure 7C, besides LiH and Al, the dehydrogenation products contain AlB_2 , which was reported as the reversible phase (Friedrichs et al., 2009). AlB_2 can accelerate the formation of LiBH_4 in the reverse reaction. The AlB_2 content was higher in $2\text{LiBH}_4\text{-Li}_3\text{AlH}_6$ than in the other samples, which signifies higher reversibility of $2\text{LiBH}_4\text{-Li}_3\text{AlH}_6$. There is an unexpected peak near 50° both in the $2\text{LiBH}_4\text{-LiAlH}_4$ and $2\text{LiBH}_4\text{-Li}_3\text{AlH}_6$ samples, which was not identified but was also detected in previous reports (Yang et al., 2007).

CONCLUSIONS

In this work, the dehydrogenation performance of three different Al source composite systems, $2\text{LiBH}_4\text{-Al}$, $2\text{LiBH}_4\text{-LiAlH}_4$, and $2\text{LiBH}_4\text{-Li}_3\text{AlH}_6$, was analyzed. Elemental Al was the raw material and was used without further purification in the $2\text{LiBH}_4\text{-Al}$ composite, in contrast to the other two samples, where it was decomposed from LiAlH_4 or Li_3AlH_6 . Li_3AlH_6 powder was prepared from LiH and LiAlH_4 . It can be concluded that the optimum synthetic conditions for ball milling are 50 h with a 25:1 ball to powder ratio at 300 rpm. The results demonstrate that Al, LiAlH_4 , and Li_3AlH_6 had a stimulative effect on LiBH_4 , allowing dehydrogenation at a relatively lower temperature. Additionally, $2\text{LiBH}_4\text{-Li}_3\text{AlH}_6$ was shown to have the best performance, with the endothermic peak of LiBH_4 at 416°C , 53°C lower than that of the pure LiBH_4 sample (469°C). The TPD results also verified the superior results of $2\text{LiBH}_4\text{-Li}_3\text{AlH}_6$, which showed the best kinetics performance among the composite samples. $2\text{LiBH}_4\text{-Li}_3\text{AlH}_6$ released 9.1 wt.% H_2 in only 150 min, which is over 95% of its theoretical hydrogen storage capacity. Its dehydrogenation product, AlB_2 , was reported as a reversible phase by researchers (Friedrichs et al., 2009), which could promote the reverse reaction of producing LiBH_4 . Further studies are needed to research the reversibility of the $2\text{LiBH}_4\text{-Li}_3\text{AlH}_6$ composite.

DATA AVAILABILITY STATEMENT

All datasets generated for this study are included in the article/supplementary material.

AUTHOR CONTRIBUTIONS

LC and YL: conception and design of study. YL and JH: acquisition of data. YL and XX: analysis and/or interpretation of data. YL: drafting the manuscript. DZ and SW: revising the manuscript critically for important intellectual content. YL, SW, DZ, JH, XX, and LC: approval of the version of the manuscript to be published.

FUNDING

This work was supported by the National Natural Science Foundation of China (51671173) and the Curriculum Reform Project (KCSZ 201809 and JGXM201912).

REFERENCES

- Carrillo-Bucio, J., Tena-García, J., and Suárez-Alcántara, K. (2017). Dehydrogenation of surface-oxidized mixtures of $2\text{LiBH}_4 + \text{Al}$ /additives (TiF_3 or CeO_2). *Inorganics* 5:82. doi: 10.3390/inorganics5040082
- Chen, J., Kuriyama, N., Xu, Q., Takeshita, H. T., and Sakai, T. (2001). Reversible hydrogen storage via titanium-catalyzed LiAlH_4 and Li_3AlH_6 . *J. Phys. Chem. B* 105, 11214–11220. doi: 10.1021/jp012127w
- Fang, F., Li, Y., Song, Y., Sun, D., Zhang, Q., Ouyang, L., et al. (2011). Superior destabilization effects of MnF_2 over MnCl_2 in the decomposition of LiBH_4 . *J. Phys. Chem. C* 115, 13528–13533. doi: 10.1021/jp203527c
- Friedrichs, O., Kim, J. W., Remhof, A., Buchter, F., Borgschulte, A., Wallacher, D., et al. (2009). The effect of Al on the hydrogen sorption mechanism of LiBH_4 . *Phys. Chem. Chem. Phys.* 11, 1515–1520. doi: 10.1039/b814282c
- He, Q., Zhu, D., Wu, X., Dong, D., Xu, M., and Tong, Z. (2019). Hydrogen desorption properties of $\text{LiBH}_4/x\text{LiAlH}_4$ ($x = 0.5, 1, 2$) composites. *Molecules* 24:1861. doi: 10.3390/molecules24101861
- Huang, X., Xiao, X. Z., Shao, J., Zhai, B., Fan, X. L., Cheng, C. J., et al. (2016). Building robust architectures of carbon-wrapped transition metal nanoparticles for high catalytic enhancement of the $2\text{LiBH}_4\text{-MgH}_2$ system for hydrogen storage cycling performance. *Nanoscale* 8, 14898–14908. doi: 10.1039/C6NR04100K
- Kou, H. Q., Xiao, X. Z., Li, J. X., Li, S. Q., Ge, H. W., Wang, Q. D., et al. (2012). Effects of fluoride additives on dehydrogenation behaviors of $2\text{LiBH}_4 + \text{MgH}_2$ system. *Int. J. Hydrogen Energy* 37, 1021–1026. doi: 10.1016/j.ijhydene.2011.03.027
- Ley, M. B., Jepsen, L. H., Lee, Y. S., Cho, Y. W., von Colbe, J. M. B., Dornheim, M., et al. (2014). Complex hydrides for hydrogen storage - new perspectives. *Mater. Today* 17, 122–128. doi: 10.1016/j.mattod.2014.02.013
- Li, Y., Xiao, X., Chen, L., Han, L., Shao, J., Fan, X., et al. (2012). Effects of fluoride additives on the hydrogen storage performance of $2\text{LiBH}_4\text{-Li}_3\text{AlH}_6$ destabilized system. *J. Phys. Chem. C* 116, 22226–22230. doi: 10.1021/jp307572x
- Liu, C., Li, F., Ma, L. P., and Cheng, H. M. (2010). Advanced materials for energy storage. *Adv. Mater.* 22, E28–E62. doi: 10.1002/adma.200903328
- Lodziana, Z., and Vegge, T. (2004). Structural stability of complex hydrides: LiBH_4 revisited. *Phys. Rev. Lett.* 93:145501. doi: 10.1103/PhysRevLett.93.145501
- Lombardo, L., Yang, H., and Züttel, A. (2019). Study of borohydride ionic liquids as hydrogen storage materials. *J. Energy Chem.* 33, 17–21. doi: 10.1016/j.jechem.2018.08.011
- Mao, J. F., Guo, Z. P., Liu, H. K., and Yu, X. B. (2009). Reversible hydrogen storage in titanium-catalyzed $\text{LiAlH}_4\text{-LiBH}_4$ system. *J. Alloys Comp.* 487, 434–438. doi: 10.1016/j.jallcom.2009.07.158
- Orimo, S. I., Nakamori, Y., Ohba, N., Miwa, K., Aoki, M., Towata, S.-I., et al. (2006). Experimental studies on intermediate compound of LiBH_4 . *Appl. Phys. Lett.* 89:021920. doi: 10.1063/1.2221880
- Schlapbach, L., and Züttel, A. (2001). Hydrogen-storage materials for mobile applications. *Nature* 414, 353–358. doi: 10.1038/35104634
- Siegel, D. J., Wolverton, C., and Ozolins, V. (2007). Thermodynamic guidelines for the prediction of hydrogen storage reactions and their application to destabilized hydride mixtures. *Phys. Rev. B* 76:134102. doi: 10.1103/PhysRevB.76.134102
- Soru, S., Taras, A., Pistidda, C., Milanese, C., Bonatto Minella, C., Masolo, E., et al. (2014). Structural evolution upon decomposition of the $\text{LiAlH}_4 + \text{LiBH}_4$ system. *J. Alloys Comp.* 615, S693–S697. doi: 10.1016/j.jallcom.2013.12.027
- Vajo, J. J. (2011). Influence of nano-confinement on the thermodynamics and dehydrogenation kinetics of metal hydrides. *Curr. Opin. Solid State Mater. Sci.* 15, 52–61. doi: 10.1016/j.cossms.2010.11.001
- Vajo, J. J., Li, W., and Liu, P. (2010). Thermodynamic and kinetic destabilization in $\text{LiBH}_4/\text{Mg}_2\text{NiH}_4$: promise for borohydride-based hydrogen storage. *Chem. Commun.* 46, 6687–6689. doi: 10.1039/c0cc01026j
- Vajo, J. J., and Olson, G. L. (2007). Hydrogen storage in destabilized chemical systems. *Scripta Mater.* 56, 829–834. doi: 10.1016/j.scriptamat.2007.01.002
- Yang, J., Sudik, A., and Wolverton, C. (2007). Destabilizing LiBH_4 with a metal (M) Mg, Al, Ti, V, Cr, or Sc) or metal hydride ($\text{MH}_2 = \text{MgH}_2, \text{TiH}_2, \text{or CaH}_2$). *J. Phys. Chem. C* 111, 19134–19140. doi: 10.1021/jp076434z
- Zhai, B., Xiao, X., Lin, W., Huang, X., Fan, X., Li, S., et al. (2016). Enhanced hydrogen desorption properties of $\text{LiBH}_4\text{-Ca(BH}_4)_2$ by a synergetic effect of nanoconfinement and catalysis. *Int. J. Hydrogen Energy* 41, 17462–17470. doi: 10.1016/j.ijhydene.2016.06.170
- Zhang, L. T., Zheng, J. G., Xiao, X. Z., Wang, X. C., Huang, X., Liu, M. J., et al. (2017). A new strategy to remarkably improve the low-temperature reversible hydrogen desorption performances of LiBH_4 by compositing with fluorographene. *Int. J. Hydrogen Energy* 42, 20046–20055. doi: 10.1016/j.ijhydene.2017.05.060
- Zhang, Y., Xiao, X., Luo, B., Huang, X., Liu, M., and Chen, L. (2018). Synergistic effect of LiBH_4 and LiAlH_4 additives on improved hydrogen storage properties of unexpected high capacity magnesium hydride. *J. Phys. Chem. C* 122, 2528–2538. doi: 10.1021/acs.jpcc.7b11222

Conflict of Interest: The authors declare that the research was conducted in the absence of any commercial or financial relationships that could be construed as a potential conflict of interest.

Copyright © 2020 Li, Wu, Zhu, He, Xiao and Chen. This is an open-access article distributed under the terms of the Creative Commons Attribution License (CC BY). The use, distribution or reproduction in other forums is permitted, provided the original author(s) and the copyright owner(s) are credited and that the original publication in this journal is cited, in accordance with accepted academic practice. No use, distribution or reproduction is permitted which does not comply with these terms.